Appl. Phys. A 84, 297–300 (2006)
DOI: 10.1007/s00339-006-3623-z

Applied Physics A
Materials Science & Processing

J.H. CHEN[1,✉]
C.P. HUANG[2]
C.G. CHAO[1]
T.M. CHEN[2]

The investigation of photoluminescence centers in porous alumina membranes

[1] Department of Materials Science and Engineering, National Chiao Tung University, Hsinchu, Taiwan 300
[2] Department of Applied Chemistry, National Chiao Tung University, Hsinchu, Taiwan 300

Received: 5 January 2006/Accepted: 27 April 2006
Published online: 1 June 2006 • © Springer-Verlag 2006

ABSTRACT To investigate the origin of blue photoluminescence (PL) in porous alumina membrane, we have prepared an anodic aluminum oxide film with a pore diameter of 40 nm in oxalic acid solution by a two-step anodization process. Our results show that the as-prepared alumina membrane is amorphous and exhibits a broad emission band peaking at around 452 nm with two sub-peaks located at 443 nm and 470 nm. As indicated by the PL excitation spectra, there are two excitation peaks which can account for the sub-peaks observed in the PL emission band. We have proposed that the broad emission band with two sub-peaks can be attributed to two luminescence centers in porous alumina membranes, namely, oxygen defects and oxalic impurities. Furthermore, we have rationalized that the two emission centers show similar influence on the PL band in the blue region based on a simple model.

PACS 81.07.-b; 81.16.Dn; 79.60.Jv

1 Introduction

Since the development of nano science and technology, research on porous alumina membranes has drawn much attention. Porous alumina is often prepared by using anodization of aluminum foils in an anodic medium [1–3], which usually contains a hexagonally packed two-dimensional array of cylindrical pores with a relatively uniform size. Due to their regular nanostructure, they have been widely used as templates for fabricating nanostructured materials, such as wires, tubes and rods for application in the fields of electronics or photoelectronics [4], magnetics [5], energy storage [6], photocatalysis [7], and biosensors [8].

Optical properties of aluminum oxide have been investigated since 1970s. Ultraviolet absorption, emission and excitation spectra were presented for high-purity crystalline alumina by Evans [9]. Crystallized alumina [10], including α-, γ-, and η phases, or sapphire [11, 12] doped with titanium and chromium ions have also revealed the optical behaviors by using various methods from the 1970's to the 1990's. Photoluminescence (PL) of porous alumina membranes was first studied in 1999. Du reported that a strong and broad PL band was observed in porous alumina membranes anodized in oxalic acid solution [13]. The mechanisms and the characterization of the PL band were complex. Therefore, there were many different explanations about this phenomenon. For example, Li et al. suggested that the PL and optical absorption in the wavelength range of 200 nm to 500 nm can be attributed to the F^+ centers in alumina membranes [14]. Gao et al. reported that the oxalic impurity was the origin of the PL emission [15].

While many studies have been done to date, more research needs to be conducted to understand the PL behavior more clearly. The present study was carried out to determine the relationship between the thickness and the PL properties of porous alumina membranes and to establish a reasonable inference to examine the phenomenon. The results of this study could be useful for providing an alternative to the mechanism of the optical properties of porous alumina membranes.

2 Experiments

General commercial aluminum foils with purity of 99.7% were used to produce porous anodic aluminum oxide templates. The aluminum sheets were first annealed for 3 h at 400° to release the mechanical stresses of the substrate and induce recrystallization. Then, porous alumina membranes were fabricated by a two-step anodizing process. In the first anodization process, the treated aluminum sheet was exposed to a 0.3 M oxalic acid solution under 40 V at 20° for 1 h. The pre-formed alumina was removed by wet etching in the mixture of phosphoric acid (6 wt. %) and chromic acid (2 wt. %) until it entirely dissolved. The sample was anodized again under the same condition for 10, 15, 20, 40 and 60 min, respectively. After the entire anodization process, the remaining aluminum was removed in a saturated $CuCl_2$-HCl (8%) solution and then cleaned thoroughly in distilled water.

The morphology and the pore size of the prepared porous alumina membranes were determined by scanning electron microscope (SEM) and atomic force microscope (AFM). The crystallinity of the aluminum oxide membranes was analyzed by X-ray diffraction (XRD, Cu K_α, $\lambda = 1.5418$ Å radiation). The fluorescence PL and PL-excitation spectra were examined at the room temperature by using a Jobin-Yvon Spex Fluolog-3 spectrophotometer with a xenon lamp as the excitation light source.

✉ Fax: +886-3-5924929, E-mail: cgchao@faculty.nctu.edu.tw

3 Results and discussion

In this study, porous alumina membranes were produced with the anodization method by a two-step process in oxalic acid solution. The porous alumina film was found to grow on aluminum with an equilibrium of oxide dissolution at the interface of the alumina/electrolyte and oxide grown at the metal/alumina interface [16]. Figure 1a shows that after the aluminum sheet was heat treated at 400° for 3 h, there is a thin oxide film on the surface of aluminum. Based on the AFM measurement results (Fig. 1b), it can be verified that the oxide is a dense alumina with a thickness about 20 nm and the roughness of 5.6 nm. As shown in Fig. 2a and b, the SEM morphology and 3D AFM image of the porous alumina membrane reveal that the pores with a diameter of 40 nm are ordered and uniform arrays.

Anodized aluminum oxide membrane was found to consist of two parts, one is a dense inner alumina barrier layer and the other is a porous outer alumina. As shown in Fig. 2c, the cross- section view of the anodized alumina membrane depicts a uniform and uninterrupted channel structure without segmentations or morphological imperfections in the porous alumina membrane. The thickness of porous alumina mem-

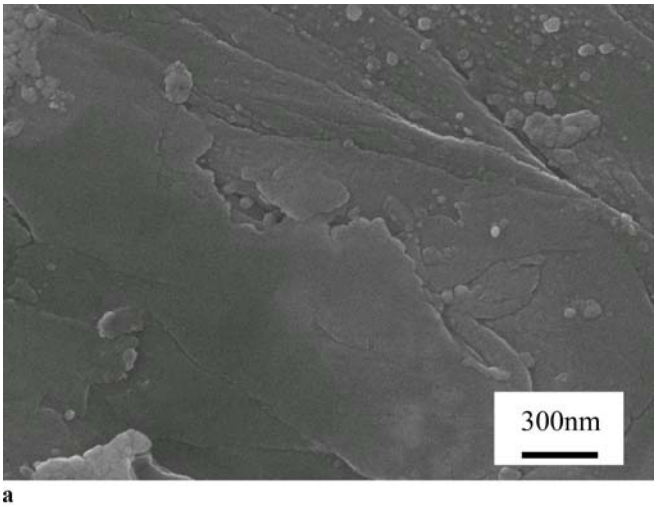

a

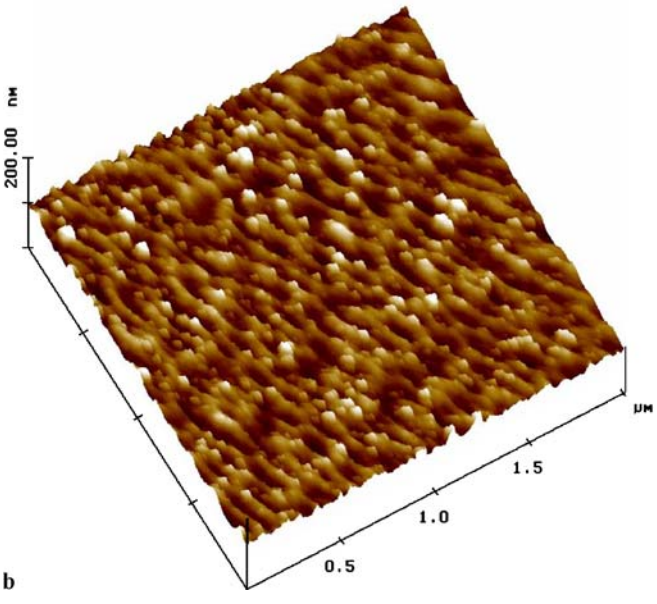

b

FIGURE 1 (**a**) SEM image of an aluminum sheet annealed and (**b**) AFM image of an aluminum sheet, both annealed at 400° for 3 h

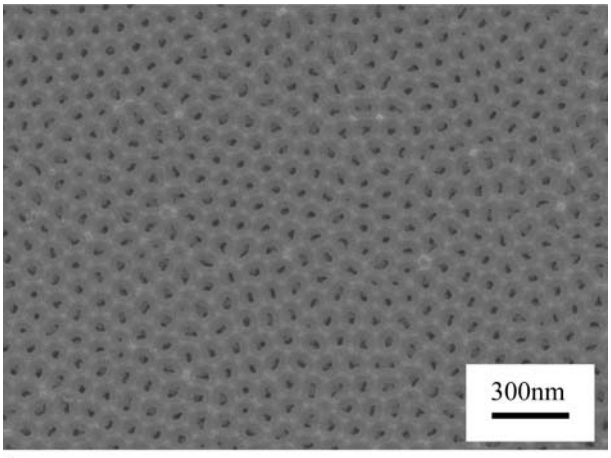

a

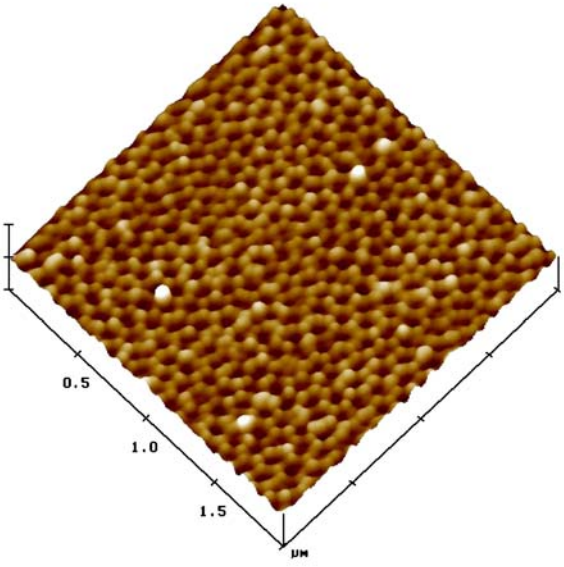

b

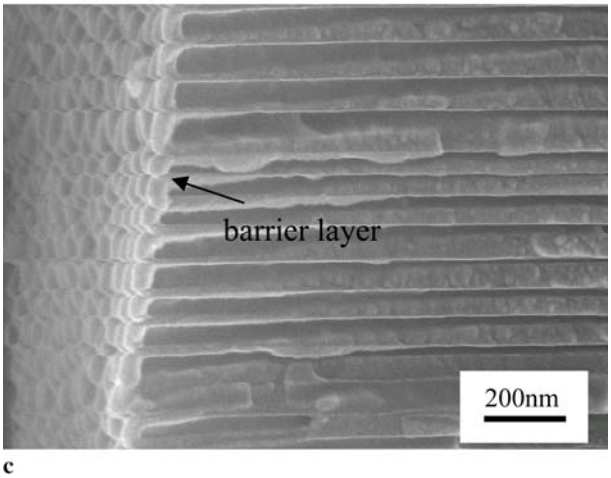

c

FIGURE 2 (**a**) SEM image of a porous alumina membrane with an ordering pore diameter of 40 nm, (**b**) 3D AFM image of the patterned surface after anodization for 60 min, and (**c**) cross section image of a porous alumina membrane

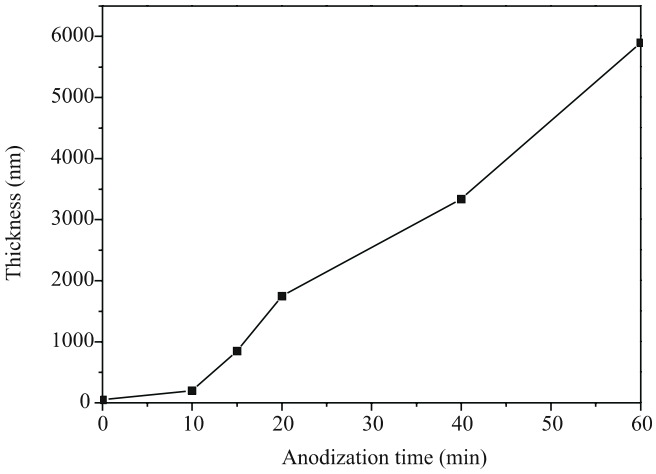

FIGURE 3 Thickness as a function of anodization time when the aluminum sheet was anodized in 0.3 M oxalic acid solution

brane was estimated from the SEM micrograph and used for estimating the growth rate of alumina membrane. The thickness of membrane is closely related proportional to the anodization time in oxalic acid solution. The growth rate of pores perpendicular to the aluminum surface was 72 nm per min, as estimated from the slope of curve shown in Fig. 3. According to the XRD analysis, the prepared porous alumina membrane is amorphous.

Figure 4a shows that the characteristic PL spectra of the dense alumina and porous alumina membranes are broad blue-emitting bands at 420–600 nm. In Fig. 4a, curve 1 peaking at 443 nm was attributed to the dense alumina on the aluminum sheet and curves 2 and 3 peaking at 470 nm can be attributed to the porous alumina membranes prepared with different anodization times (10–15 min) on aluminum sheets in oxalic acid solution. When the anodization time was longer than 15 min (e.g., 15–60 min), the emission band was found to be broad centered at 452 nm, as shown in curves 3 to 6. As the thickness of the porous alumina membrane increases, the peak intensity of the emission band increases gradually and the peak position changes obviously. Moreover, the dense alumina and the porous alumina membranes have different emission centers, which induce a red shift for the PL emission peaks. As indicated by the results, both the thickness of porous alumina membranes and the PL intensity were found to increase with increasing anodization times.

The PLE spectra monitored at 440 nm (line+symbol) and 470 nm (symbol) and measured in the 200–400 nm spectra range for porous alumina membranes were presented in Fig. 4b. When the anodization time is shorter than 15 min (curves 1–3), the PLE spectra monitored at 440 nm exhibit two excitation centers located at 343 and 360 nm, respectively, except for the curve of the dense alumina which only shows a vague peak at around 343 nm. Furthermore, the intensity of the excitation band grows steadily and the center positions remain unshifted at around 350 nm when the anodization time exceeds 15 min (curves 4–6). The spectra monitored at 470 nm are similar to theirs monitored at 440 nm but there is a red shift in the excitation spectra. The results could be explained by considering the emission peaks located at 443 nm and 470 nm. There is a red shift between the two emission peaks. Therefore, it is reasonable that a red shift appears in the excitation spectra monitored at 440 nm and 470 nm. These findings seem inconsistent with the observed blue emission, which occur at 443 and 470 nm may be attributed to the different excitation centers.

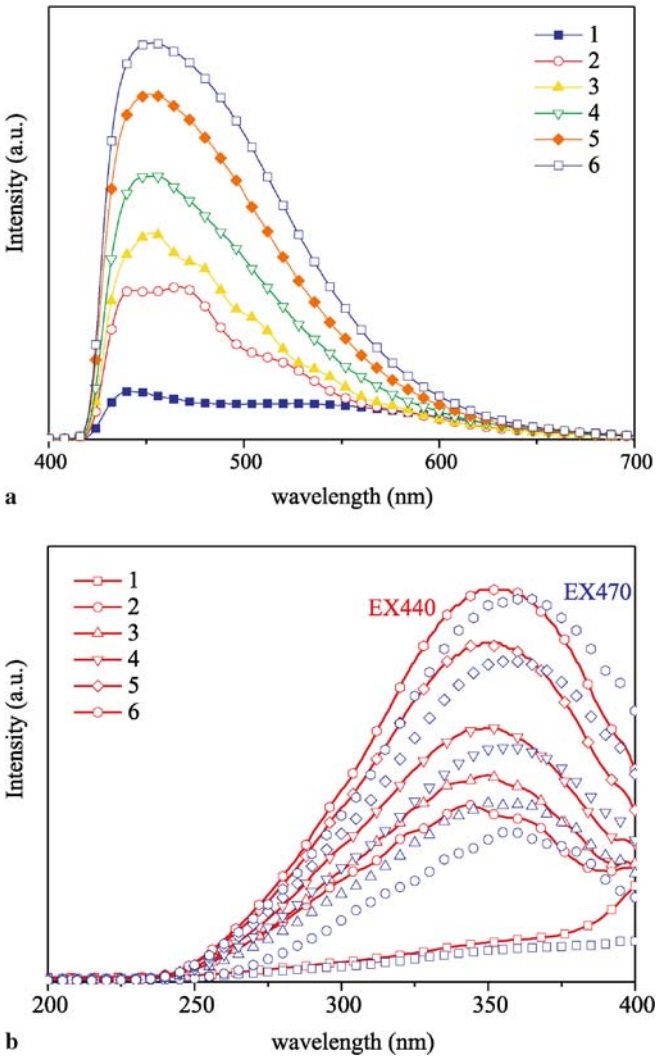

FIGURE 4 PL spectra (**a**) and excitation spectra (**b**) of the aluminum sheet and porous alumina membranes prepared in oxalic acid solution. 1: annealed aluminum; 2: anodized 10 min; 3: anodized 15 min; 4: anodized 20 min; 5: anodized 40 min; 6: anodized 60 min

The mechanisms of photoluminescence for porous alumina membranes have been studied by several researchers. Du et al. [13] and Huang et al. [17] reported that a blue-emitting PL band was originated from ionized oxygen deficient defect centers of the alumina membrane occurring in the wavelength range of 400–600 nm. The density of the oxygen defects in the alumina membrane was found to increase by increasing the depth of pore walls. Gao and coworkers [15] suggested that the oxalic impurities rather than F^+ was responsible for blue luminescence at 470 nm observed in the alumina membrane. We could conclude with certainty that both studies are able to explain significant variance of PL spectra. A thin dense alumina film without oxalic impurities forms after the aluminum foil is annealed at 400°. The emission center of this dense alumina is observed only at the

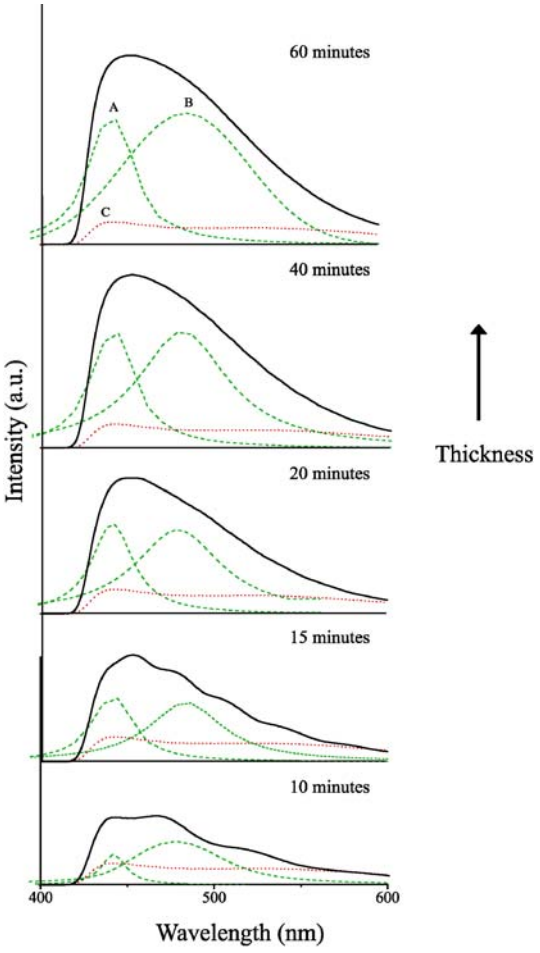

FIGURE 5 Schematic diagram for PL curve of the porous alumina membranes whose spectra have been deconvoluted by Gaussian functions (A and B curves) and the dense alumina (C curve)

wavelength of 443 nm, which can be attributed to the oxygen defects. However, when the sample is anodized in oxalic acid solution, the other emission appears at around 470 nm which is in agreement with the results obtained from Gao et al. [15]. At the mean time, there is also the oxygen vacancies produced in the porous alumina membrane during the anodization process. The concentrations of the oxygen defects and the oxalic impurities were found to increase with increasing anodization time, and thus, the intensities of both peaks increase gradually. The experimental spectra of the porous alumina membranes have been deconvoluted by Gaussian functions into two emission bands, as showed in Fig. 5. The schematic diagram adequately describes the PL behavior in terms of three components, namely, the oxygen defects (A, located at 443 nm), the oxalic impurities (B, located at 470 nm) and the dense alumina of the substrate (C). The emission wavelength of the porous alumina membranes with different thicknesses was observed to exhibit remarkable changes due to the combination of A, B and C curves. Although the emission intensity is amplified, the integrated emission contribution of two fitting peaks is invariable with the ratio of 1 to 1. Therefore, we propose that the PL emission band can be attributed to two sources, one at 443 nm is correlated with the oxygen vacancies and the other at 470 nm is originated from the oxalic impurities.

4 Conclusion

Porous alumina membranes were produced by anodization method by adopting a two-step anodization process in oxalic acid solution. X-ray analysis indicates that the alumina membrane was amorphous phase. As indicated by the PL emission spectra, the intensity of PL band increases with increasing thickness of alumina membranes determined from SEM figures. The emission wavelength shifts from 443 nm to 443 nm and 470 nm, and finally located around 452 nm as the thickness of porous alumina membranes increases. The PL excitation spectra are found to be consistent with the above changes from a broad peak to two peaks. A part of the explanation for these may lie in the fact that there are two emission centers caused by oxygen vacancies and oxalic impurities in the PL band. According to deconvolution of the PL spectra, both centers contribute greatly to the PL emission band. This study has taken a step in the direction of defining the relationship between the thickness and the photoluminescence in porous alumina membranes. In addition, it is important to emphasize that the variety of oxygen vacancies and oxalic impurities. Future studies will address the coupling of these centers to excitons. The application of porous alumina membranes as two dimensional photonic crystals or micropolarizers has been noted recently. Therefore, more extensive researches would be necessary to make definite claims in these fields.

ACKNOWLEDGEMENTS This work was supported by the National Science Council of the Republic of China under Research Contract No. NSC94-2216-E009-003.

REFERENCES

1 M.T. Wu, I.C. Leu, M.H. Hon, J. Vac. Sci. Technol. B **20**, 776 (2002)
2 S. Shingubara, K. Morimoto, H. Sakaue, T. Takahagi, Electrochem. Solid State Lett. **7**, E15 (2004)
3 N. Stein, M. Rommlfangen, V. Hody, L. Johann, J.M. Lecuire, Electrochim. Acta **47**, 1811 (2002)
4 Y. Huang, X. Duan, Y. Gui, C.M. Lieber, Nano Lett. **2**, 101 (2002)
5 K. Nielsch, F. Muller, A.P. Li, U. Gosele, Adv. Mater. **12**, 582 (2002)
6 G.L. Che, B.B. Laksshmi, E.R. Fisher, C.R. Martin, Nature **393**, 346 (1998)
7 S.Z. Chu, S. Inoue, K. Wada, D. Li, H. Haneda, J. Mater. Chem. **13**, 866 (2003)
8 F. Matsumoto, K. Nishio, H. Masuda, Adv. Mater. **16**, 2105 (2004)
9 B.D. Evans, M. Stapelbroek, Phys. Rev. B **18**, 7089 (1978)
10 B.G. Draeger, G.P. Summers, Phys. Rev. B **19**, 1172 (1979)
11 P. Lacovara, L. Esterowitz, M. Kokta, IEEE J. Quantum Electron. **QE-21**, 1614 (1985)
12 W. Chen, H. Tang, C. Shi, J. Deng, J. Shi, Y. Zhou, S. Xia, Y. Wang, S. Yin, Appl. Phys. Lett. **67**, 317 (1995)
13 Y. Du, W.L. Cai, C.M. Mo, J. Chen, L.D. Zhang, X.G. Zhu, Appl. Phys. Lett. **74**, 2951 (1999)
14 Y. Li, G.H. Li, G.W. Meng, L.D. Zhang, F. Phillipp, J. Phys.: Condens. Matter **13**, 2691 (2001)
15 T. Gao, G. Meng, L. Zhang, J. Phys., Condens. Matter **15**, 2071 (2003)
16 O. Jessensky, F. Muller, U. Gosele, Appl. Phys. Lett. **72**, 1173 (1998)
17 G.S. Huang, X.L. Wu, Y.F. Mei, X.F. Shao, G.G. Siu, J. Appl. Phys. **93**, 582 (2003)